J. Mod. Power Syst. Clean Energy (2016) 4(2):248–255
DOI 10.1007/s40565-015-0156-5

Probabilistic equivalent model of DFIG-based wind farms and its application in stability analysis

Haiqiang ZHOU[1], Ping JU[1], Yusheng XUE[2], Jie ZHU[1]

Abstract A probabilistic equivalent method for doubly fed induction generator (DFIG) based wind farms is proposed in this paper. First, the wind farm equivalent model is assumed to be composed of three types of equivalent DFIGs with different dynamic characteristics. The structure of equivalent model remains constant, whereas the parameters change with the migration of different scenarios in the wind farm. Then, historical meteorological data are utilized to investigate the probability distribution of key equivalent parameters, such as capacity, wind speed and electrical impedance to the point of common coupling. Each type of equivalent DFIG is further clustered into several groups according to their active power output. Combinations are created to generate representative scenarios. The probabilistic equivalent model of wind farm is finally achieved after removing invalid combinations. Most matched representative scenarios can be predicted according to the real-time measurement. The equivalent model is applied to the probabilistic power flow calculation and the stability analysis of test systems.

Keywords Doubly fed induction generator (DFIG), Wind farm, Probabilistic equivalent model, Representative scenarios, Stability analysis

CrossCheck date: 17 May 2015

Received: 26 August 2014 / Accepted: 18 May 2015 / Published online: 14 October 2015

✉ Haiqiang ZHOU
js.hq@163.com

Ping JU
pju@hhu.edu.cn

Yusheng XUE
xueyusheng@sgepri.sgcc.com.cn

Jie ZHU
zhujiewinni@163.com

[1] Hohai University, Nanjing 210098, China

[2] State Grid Electric Power Research Institute, Nanjing 210003, China

1 Introduction

In recent years, wind generation has experienced a rapid growth in China. By the end of 2013, the total capacity of wind generation installations reached 75.48 GW, and the total power generated by wind in the same year was 140. 1 billion kWh. The output of wind farms fluctuates significantly. The system frequency may experience large fluctuations if the system reserve is inadequate or its dynamics is not fast enough. Wind generators absorb large amounts of reactive power from the grid during fault times, and this situation is detrimental to voltage recovery. These problems pose great challenges to power system security, especially when the penetration ratio of wind generation is high. To guarantee the system security, analyzing system stability and studying available controls thoroughly are very important [1–3].

Presently, doubly fed induction generators (DFIGs) have become the most commonly used type of wind generators because of their technical and economic performance [4, 5]. This paper focuses on DFIG-based wind farms and all DFIGs in wind farms are assumed to be the same type with identical parameters.

A wind farm may consist of hundreds or even thousands of DFIGs. Sometimes many wind farms dispersed in a wide range are integrated into a large-scale interconnected power system. In this situation, each wind farm can be

STATE GRID
STATE GRID ELECTRIC POWER RESEARCH INSTITUTE

described with an equivalent DFIG. The total wind generation may be regarded as a virtual wind plant which composes many equivalent DFIGs. Wind speed and directions differ one from another and the wind farm cannot be analyzed with detailed models because of the well-known 'dimension catastrophe' problem. The equivalent model is an effective method for reducing system order. However, the equivalent model is usually calculated at a specific steady state. The environmental scenario of wind farms keeps changing, and the steady state drifts due to the unpredictability of wind. Therefore, the equivalent model based on the operation point is stochastic; both structures and parameters of the equivalent model are random. Conclusions under different scenarios will also be different.

The common methods used to deal with system randomness are the Monte Carlo method and the analytical method. The Monte Carlo method produces a large number of samples through random sampling. Each sample is analyzed, and the results are obtained through statistical analysis. The analytical method combines the semi-invariant and Gram–Charlier expansions to calculate the joint probability distribution density function [6]. The mechanism of the Monte Carlo method is simple, but the computation tasks are heavy. For example, if the wind farm consists of 10 DFIGs of the same type, and the wind speed of each generator has only 10 possible values, the number of possible scenarios will be 10 billion. Investigating such a large sample set is practically impossible. The analytical method is based on probability theory, and analysis is performed close to a steady-state operation point. Research shows that the analytical method is less accurate than the Monte Carlo method and needs to be improved.

This paper proposed a novel method of building the probabilistic equivalent model of DFIG wind farms. The wind farm was clustered and aggregated, and consisted of three equivalent DFIGs of different dynamical characteristics. The structure remained constant under various scenarios while the equivalent parameters changed. All historical scenarios were aggregated and investigated. Each type of equivalent DFIG was classed into several groups according to their dynamic characteristics and was approximated by representative DFIGs. Combinations of representative DFIGs were performed to generate all possible representative scenarios. Then, the wind farm was simulated by representative scenarios and their probability distribution function (PDF). The most matched scenarios could be found according to the real-time measurement. Finally, the model was validated through simulations of the test system. The probabilistic power flow coincides well before and after the equivalent. The damping ratios of the system under different scenarios were also studied.

This paper is organized as follows: Section 2 introduces the aggregation method of DFIG-based wind farms. The structure, clustering criterion, and calculations of equivalent parameters are given. Section 3 presents the probabilistic equivalent model, and the generation of representative DFIGs and representative scenarios are both introduced. The applications of the probabilistic equivalent model are discussed in Section 4. Section 5 presents case studies. The model was applied in the probabilistic power flow calculation and stability analysis of the test system. Conclusions are given in Section 6.

2 DFIG-based wind farm equivalent

DFIGs under different wind speeds work with different control strategies, namely, starting, maximum power point tracking, constant speed, and constant power. They show distinct dynamics. DFIGs are usually clustered into several groups according to wind speed or rotor speed [7]. However, considering only wind speed in clustering is insufficient because the dynamics of the DFIG is also affected by the structure of the power system. Dynamical impacts of the wind farm to external power system can be observed at the point of common coupling (PCC). The post-fault voltage at the PCC and injected reactive power vary little under different wind speeds. The major difference lies in the active power responses. It was shown in [8] that the dynamics of a DFIG mainly depended on its capacity, wind speed, and the impedance to the PCC. The output of the DFIG varies significantly when the impedance to PCC changes, even if capacity and wind speed remain constant.

DFIG is a special type of induction generator. DFIGs can be described with a third order model as induction motors [9]. The dynamics characteristics of DFIG are similar to those of induction motor. It was shown in [10] that two types of equivalent induction motors were sufficient to get a good accuracy for the equivalent model of motors in power system. Three typical post-fault responses of DFIGs under different wind conditions are shown in Fig. 1. According to [8], three types of equivalent DFIGs got a good precision. Thus, three types of equivalent DFIGs are applied in the aggregation of the wind farm. More types of equivalent DFIGs may result in a better accuracy, but also increase the computation tasks largely.

As a nonlinear system, providing an analytical form-clustering criterion for DFIGs is difficult. However, for a special wind farm, the clustering criterion may be achieved by offline numerical simulations and can be expressed in a diagram, and can be applied through a lookup table in aggregation. As capacities were assumed to be the same,

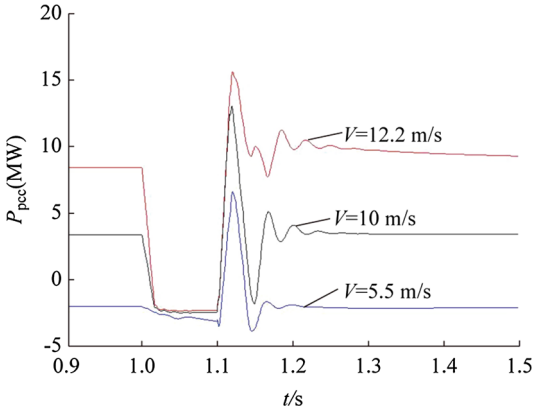

Fig. 1 Three types of responses of DFIG active power with different scenarios

the clustering criterion will only be determined by wind speed and the impedance to PCC. The criterion for the test system in Section V is shown in Fig. 2. Regions 1, 2, and 3 are areas classed according to wind speed and impedance to PCC. The DFIGs, whose parameters are located in Regions 1, 2, and 3, are working at slow, moderate, and fast wind speeds respectively. Their dynamic characteristics are similar to those shown in Fig. 1. The boundary between Region 1 and 2 varies slightly when the impedance increases, but when the impedance between DFIG and PCC increases sufficiently, the boundary between Region 2 and 3 disappears. The pitch angle control system takes effect when the wind speed increases but the electrical connection to PCC is weak. As such, the DFIG exhibits different dynamics.

According to the clustering criterion shown in Fig. 2, the DFIGs in the wind farm can then be clustered into three groups. DFIGs in one group may be aggregated to an equivalent DFIG with similar methods of induction motor aggregation. For DFIGs of the same type, the parameters of the equivalent DFIG in per unit (taken its capacity as the base value) is equal to that of a single DFIG. Thus, the dynamics of a DFIG-based wind farm can be represented by three equivalent DFIGs. The structure of the equivalent model is shown in Fig. 3. The structure remains constant, whereas the parameters of equivalent DFIGs vary when the system works under different scenarios. The unpredictability of the wind farm's environmental scenario is depicted by the probability distribution of the equivalent DFIG parameters.

In Fig. 3, the equivalent wind speeds v_{equ_i} (i = 1, 2, 3) can be deduced by the law of conservation of energy, which means the total mechanical output power remains constant before and after the equivalent. The impedance to PCC Z_{equ_i} can be calculated based on the Thevenin equivalent circuit method when the DFIG is treated as a voltage source behind the transient impedance [8, 9]. The equivalent capacity S_{equ_i} equals n_iS, where S is the capacity of a single DFIG, and n_i is the number of DFIGs in the group.

The parameters of $DFIG_{equ\_i}$ can be expressed by

$$\boldsymbol{C}_i = \left(n_i S,\ v_{equ\_i},\ Z_{equ\_i}\right) \tag{1}$$

Clearly, the dynamics of $DFIG_{equ\_i}$ is determined by parameter vector C_i, while the wind farm dynamics is determined by $\boldsymbol{C} = \{\boldsymbol{C}_1, \boldsymbol{C}_2, \boldsymbol{C}_3\}$. Every scenario will have a distinct evaluation of $\boldsymbol{C}^{(k)}$. The superscript 'k' denotes the scenario, and the subscript 'i' denotes the type of equivalent DFIG.

3 Probabilistic equivalent model of wind farm

Theoretically, the probabilistic equivalent model of a DFIG wind farm can be depicted by the PDF of vector $\boldsymbol{C}$. The PDF can be obtained by investigating the original samples. A detail that should be pointed out, however, that

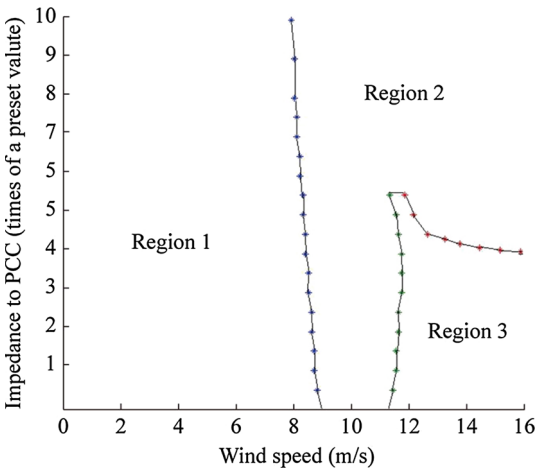

Fig. 2 Clustering criterion of test wind farm

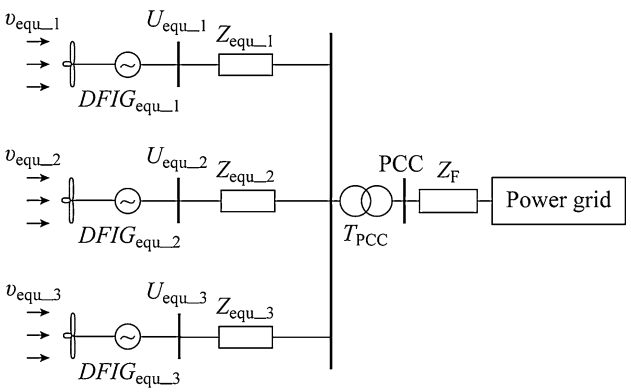

Fig. 3 Equivalent model of DFIG wind farm

the doubly fed wind farm equivalent model consists of three equivalent DFIGs and that nine elements are present in parameter vector $\boldsymbol{C}$. Even if only five possible values exist for each element, the total number of possible samples of $\boldsymbol{C}$ will reach 1.953 million (5^9). The historical meteorological data were utilized in the analysis. If the wind speeds were recorded every 15 minutes, a total of 35040 scenarios would be recorded in a year. The original samples $\{S^{(k)},\ k = 1,2,\cdots,35040\}$ are insufficient for statistical analysis of such a large set as $\boldsymbol{C}$. Some scenarios may not be included in the original samples. Even the computation and analysis of 35040 samples was difficult to complete. A reduction of the original samples is needed.

The purpose of the reduction is to approximate the original samples with a small number of representative scenarios and their probabilities distributions, while most of the dynamical characteristics of the wind farm are kept in the means of statistics. Indeed, many scenarios have similar dynamics, and representative scenarios can describe them. The PDF of the three equivalent DFIGs can be analyzed separately. Strictly speaking, the similarity between two equivalent DFIGs under scenarios $S^{(j)}$ and $S^{(k)}$ should be measured by the dynamic responses at PCC after disturbances. The dynamics of $DFIG_{\text{equ}\_i}$ is determined by vector $\boldsymbol{C}_i$. Therefore, the similarity can be measured by $\left\|\boldsymbol{C}_i^{(j)} - \boldsymbol{C}_i^{(k)}\right\|$. A smaller distance between $\boldsymbol{C}_i^{(j)}$ and $\boldsymbol{C}_i^{(k)}$ corresponds to greater similarity between the two DFIGs. As the parameters of $DFIG_{\text{equ}\_i}^{(j)}$ and $DFIG_{\text{equ}\_i}^{(k)}$ are located in the same region in Fig. 2, $DFIG_{\text{equ}\_i}^{(j)}$ and $DFIG_{\text{equ}\_i}^{(k)}$ will clearly have similar dynamics. The only difference lies in the output of the equivalent DFIG.

The output of $DFIG_{\text{equ}\_i}$ is affected by wind speed and capacity. The relationships between the output and the two parameters of equivalent DFIGs in the test system are shown in Fig. 4. The outputs increase gradually when v_{equ_i} and n_i increase. Different evaluations of $\boldsymbol{C}_i$ with the same output may exist, especially for $DFIG_{\text{equ}\_1}$. To reduce computation tasks, we further class $DFIG_{\text{equ}\_i}$ into m_i groups according to their output, that is, the output of $DFIG_{\text{equ}\_i}$ is divided into m_i intervals. The equivalent DFIGs whose outputs fall into one interval will be approximated by a representative equivalent DFIG. The output of this representative DFIG is evaluated by the mean output of all equivalent DFIGs located in this interval. Thus, $DFIG_{\text{equ}\_i}$ representative DFIGs are chosen to depict all the possible dynamical characteristics of $DFIG_{\text{equ}\_i}$.

The number m_i is determined according to the PDF of the output. If the probability of output in an interval is high, then more intervals may be needed to reduce error. From the point of view of physical mechanism, aggregating v_{equ_i} into three or four typical values and classing the capacities into roughly three types may lead to a precise result. Roughly 10 representative DFIGs will be enough to describe typical dynamics

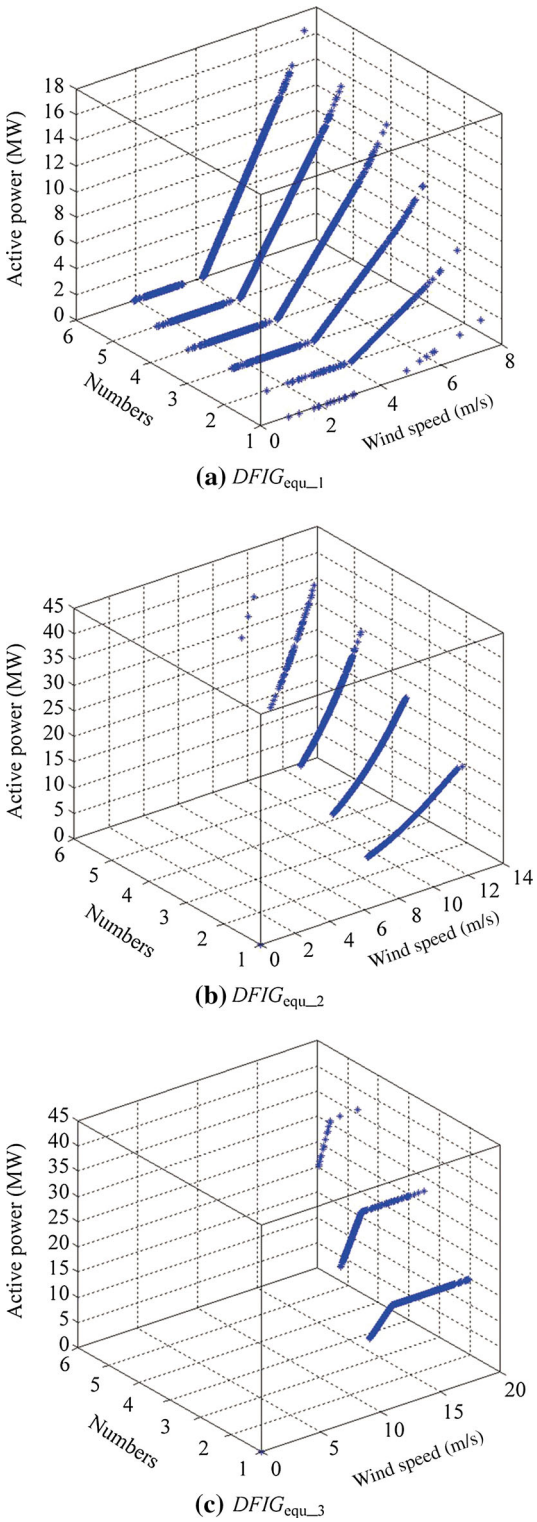

Fig. 4 Relationships of outputs, wind speeds, and capacities of three equivalent DFIGs

for a kind of equivalent DFIG. m_1, m_2 and m_3 have often been suggested to be set to 6, 5, and 4, respectively, and they can be adjusted according to the demand of model accuracy. The accuracy of representative models will increase when m_1, m_2 and m_3 increase. However, the computation tasks will also increase.

The equivalent model of wind farm consists of three equivalent DFIGs. The $m_1m_2m_3$ representative scenarios can be obtained through combinations. Given the constraint that sum capacity does not change, some combinations are in fact invalid and should be removed. Thus, the number of valid representative scenarios n_r is less than $m_1m_2m_3$. The probability of each representative scenario can be evaluated by the cumulative probability. Therefore, the probabilistic equivalent model of DFIG wind farm $\{\bar{\boldsymbol{C}}^{(k)},\ p_k;\ k = 1,\ 2, \cdots, n_r\}$ is achieved.

In summary, the steps to probabilistic equivalent of DFIG-based wind farm are as follows:

1) The wind farm is aggregated under historical scenarios $\{S^{(k)}, k = 1,\ 2, \cdots, n_S\}$. The equivalent model of wind farm is constructed with three types of equivalent DFIGs.
2) The original samples $\{\boldsymbol{C}_i^{(k)}, k = 1,\ 2, \cdots, n_S\}$ $(i = 1,\ 2,\ 3)$ are generated for each type of equivalent DFIG.
3) $DFIG_{\text{equ}\_i}$ is classed into m_i groups according to their outputs. The mean output of each interval is calculated, and the m_i representative DFIG models $\{\bar{\boldsymbol{C}}_i^{(k)}, k = 1,\ 2, \cdots, m_i\}$ for $DFIG_{\text{equ}\_i}$ are identified.
4) Combinations of the representative DFIGs of the three equivalent DFIGs. Invalid combinations are removed. The cumulative probability of each representative scenario is calculated by investigating the original samples. The probabilistic equivalent model $\{\bar{\boldsymbol{C}}^{(k)}, p_k;\ k = 1,\ 2, \cdots, n_r\}$ of the wind farm is obtained.
5) The power system is analyzed with probabilistic equivalent model.

The number of the representative models is unrelated to the scale of the wind farm and the number of the original scenarios. The equivalent reduces computation tasks significantly while retaining most of the characteristics. Certainly, the reduction will introduce some errors, but considering the counteraction effect of errors of three equivalent DFIGs, the total errors will be very small. The probabilistic model should be updated with the increase of n_s to retain its representative.

4 Applications in probabilistic stability analysis

Based on the probabilistic equivalent model of wind farms, the stability of power system can be analyzed. The electromechanical oscillations after disturbance were analyzed. The attenuation factors α, frequencies f, and minimum damping ratio $\xi_{\min}$ of the dominant oscillation modes can be calculated [11–13]. The Prony algorithm may be used in the analysis of a large-scale system. The PDF of the minimum damping $P(\xi_{\min})$ can be found according to the PDF of representative scenarios. The stability analysis results can be applied in the design of controllers.

If m_1, m_2 and m_3 are set to the suggested values, then the number of the representative models will be less than 120 ($6 \times 5 \times 4$). The number of scenarios can be further reduced according to the measured power $P_{\text{PCC},m}$ injected to power grid at the PCC. Each representative scenario $\bar{\boldsymbol{C}}^{(k)}$ has its injected power $P_{\text{PCC}}^{(k)}$. Evidently, the current scenario matches $\bar{\boldsymbol{C}}^{(k)}$ well when $|P_{\text{PCC},m} - P_{\text{PCC}}^{(k)}|$ is small. In practice, the probability that current scenario matches a representative model $\bar{\boldsymbol{C}}_i^{(k)}$could be calculated by (2).

$$Prob(\boldsymbol{C}_{\text{curr}} \text{ matches } \overline{\boldsymbol{C}}^{(k)}) = \begin{cases} \dfrac{p_k}{\sum\limits_j p_j} \exp\left(-\left|P_{\text{PCC},m} - P_{\text{PCC}}^{(k)}\right|\right), & j \in \left\{\left|P_{\text{PCC},m} - P_{\text{PCC}}^{(j)}\right| \le \varepsilon\right\} \\ 0, & \left|P_{\text{PCC},m} - P_{\text{PCC}}^{(k)}\right| \ge \varepsilon \end{cases} \tag{2}$$

The probability is an inverse exponential function of $\left|P_{\text{PCC},m} - P_{\text{PCC}}^{(k)}\right|$ and is also proportional to p_k, i.e., the probability of $\bar{\boldsymbol{C}}_i^{(k)}$. The ε in (2) is a preset value. Generally, it may be three or four times the capacity of a single DFIG. If $\left|P_{\text{PCC},m} - P_{\text{PCC}}^{(k)}\right| \ge \varepsilon$, then the probability is seen to be zero. The representative scenarios may be sorted according to their probabilities, and the most matched representative scenarios can be found. Usually less than twenty representative scenarios will be retained for detailed analysis.

5 Case studies

Simulations were conducted in the test system to validate the effectiveness of the probabilistic equivalent model of wind farms. The diagram of the test system is shown in Fig. 5 and is based on the Western systems coordinating council (WSCC) system proposed in [14]. A wind farm is connected to bus 9 through step-up transformers. Bus 10 is the PCC, and bus 1 is the slack bus. The wind farm consists of sixty DFIGs. For simplicity, these DFIGs were represented by six DFIGs whose capacity is ten times the capacity of a single machine, whereas the wind speed is the same. The parameters of a single DFIG are given in Appendix 1, and the wind farm data are given in Appendix 2. The wind speed data of a wind farm located in Jiangsu

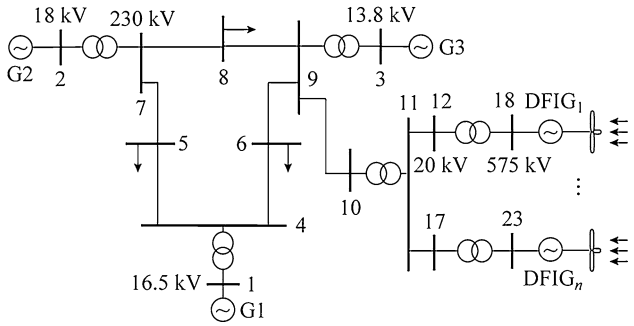

Fig. 5 WSCC system integrated with DFIG-based wind farm

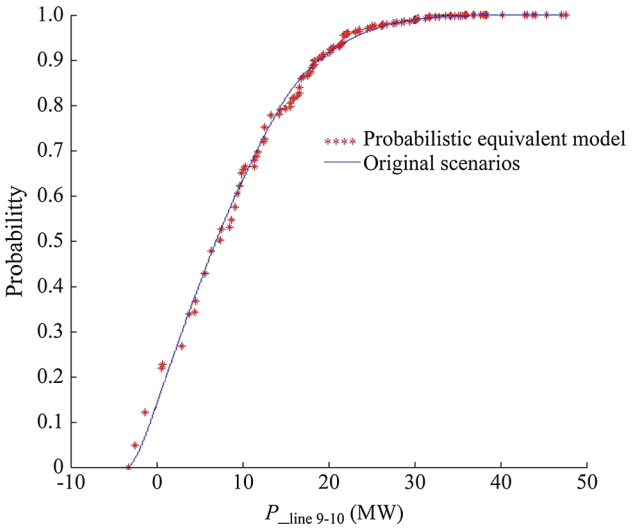

Fig. 6 Comparisons of power flow PDF between original scenarios and probabilistic equivalent model

Province were taken as example. The wind data of 2008 were taken for study. They were recorded every 15 minutes. The test system was simulated using the MATLAB/Simulink toolbox.

5.1 Probabilistic equivalent model

Probabilistic equivalent method was applied in the test system. The m_1, m_2 and m_3 were set to 7, 6, and 5, respectively. The output of $DFIG_{\text{equ\_1}}$ falls into [0, 15] MW, and was classed into seven intervals: ① Nonexistent; ② Equivalent wind speed is too slow to start; ③ $P \in (0, 1.5]$; ④ $P \in (1.5, 3.0]$; ⑤ $P \in (3.0, 5.0]$; ⑥ $P \in (5.0, 7.5]$; ⑦ $P > 7.5$.

Similarly, the output of $DFIG_{\text{equ\_2}}$ was classed into six intervals: ① Nonexistent; ② $P \leq 7.5$; ③ $P \in (7.5, 10]$; ④ $P \in (10, 15]$; ⑤ $P \in (15, 25]$; ⑥ $P > 25$.

Finally, the output of $DFIG_{\text{equ\_3}}$ was classed into five intervals: ① Nonexistent; ② $P \leq 15$; ③ $P \in (15, 22]$; ④ $P \in (22, 30]$; ⑤ $P > 30$.

Each representative equivalent DFIG was calculated. Then, 210 ($7 \times 6 \times 5$) possible representative scenarios were obtained through combinations of these representative DFIGs, and invalid combinations were removed. A total of 135 representative scenarios and their probabilities were chosen as the probabilistic equivalent model of the wind farm. Due to space limitations, the detailed results are not listed in this paper.

5.2 Probabilistic power flow

The active power of the tie line from bus 9 to bus 10 was observed to validate the PDF of power flow before and after equivalent. The comparison is shown in Fig. 6. The mean output and variance calculated by the equivalent scenarios were 8.3703 and 7.7684, respectively, while the values calculated by the original scenarios were 8.6282 and 7.6922, respectively. The two PDF curves fit well. The power flows in other lines in the system are also observed. They both proved that the statistical characteristics in steady states are retained well by the probabilistic equivalent model.

5.3 Probabilistic stability analysis and online model match

The small signal analysis (SSA) of the test system was studied based on the probabilistic equivalent model. A three-phase short circuit fault at bus 9 was studied. The fault occurred at 1 s and was cleared at 1.1 s. In total, 135 representative scenarios were simulated. The Prony algorithm was used to analyze the swings of rotor angles of generators G2 and G3. The PDF of damping ratios of generators G2 and G3 are shown in Fig. 7. Each generator has two dominant oscillation modes, one with a frequency of about 1.4 Hz and the other with a frequency of about 2.2 Hz. Moreover, the damping of the low-frequency oscillation mode is lower than that of the high-frequency mode. In general, the damping ratio of generator G2 is higher than G3. The minimum damping ratios fall under 0.03 under some scenarios, which is dangerous for system security. Control strategies such as the power system stabilizer should be considered to improve system stability.

If the active power of line 9 to line 10 was measured in real time, for example, then it would have been 11.5 MW with ε set to 5 MW. Twenty-six representative models were found to be possible matches with the current scenario. The probability varied from 0.1262 to 0.0005. Among them, the probabilities of 19 models were higher than 0.005. The most matched three representative scenarios and their probabilities are listed in Appendix 3.

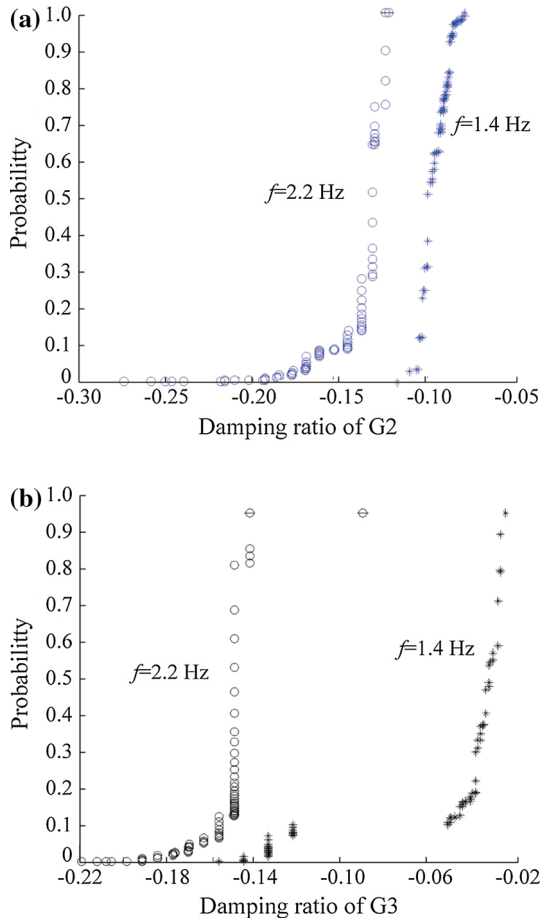

Fig. 7 Oscillation modes damping ratio PDF of G2 and G3 rotor angles

6 Conclusions

In this paper, the probabilistic equivalent model of DFIG wind farms is assumed to be composed of three types of equivalent DFIGs. The structure of the equivalent model remains constant, while the parameters change in different scenarios. Wind speed, electrical distance to the PCC, and capacity are dominant parameters of a DFIG. Each type of equivalent DFIG may be depicted by several representative DFIGs. The representative scenarios are obtained by combinations, and the PDF can be obtained by investigation about the original scenarios. This study shows that steady and dynamical characteristics are preserved well by the probabilistic equivalent model. It can reduce computation tasks significantly while maintaining the impact in the means of statistics. Subsequent research will focus on the application of this model in controller optimization of wind power systems.

Acknowledgment This work was supported by the Special Fund of the National Priority Basic Research of China (No. 2013CB228204) and the National Science Foundation of China (No. 50977021).

Appendix 1: DFIG parameters

$D = 0.01$; $R_s = 0.00706$; $R_r = 0.005$; $X_m = 2.9$; $X_{\sigma s} = 0.171$; $X_{\sigma r} = 0.156$; $V_{DC} = 1200$ V; the rated power is 1.5 MW, the rated voltage is 575 V; the inertia is 10.08 s; the DC link capacitor is 10000 μF.

Appendix 2: Wind farm network data

Wind farm network data are

$$Z_{9\_10} = 0.001 + \mathrm{j}0.0058,$$
$$Z_{11-12} = Z_0, Z_{11-13} = 2Z_0, Z_{11-14} = 3Z_0, Z_{11-15} = 4Z_0,$$
$$Z_{11-16} = 5Z_0, Z_{11-17} = 6Z_0, Z_0 = 0.0084 + \mathrm{j}0.0495;$$
$$Z_{T10-11} = 0.0053 + \mathrm{j}0.05; (S_{base} = 100\mathrm{MVA})$$

$$Z_{T12-18} = 0.0017 + \mathrm{j}0.05, Z_{T13-19} = 0.0017 + \mathrm{j}0.05,$$
$$Z_{T14-20} = 0.0017 + \mathrm{j}0.05, Z_{T15-21} = 0.0017 + \mathrm{j}0.05,$$
$$Z_{T16-22} = 0.0017 + \mathrm{j}0.05, Z_{T17-23} = 0.0017 + \mathrm{j}0.05.$$
$$(S_{base} = 20\mathrm{MVA}).$$

Appendix 3: Most matched three scenarios for $P_{\text{line9-10}} = 11.5$ MW

Scenario 1:

$$\boldsymbol{C}_1 = (75\,\mathrm{MW}, 5.5057\,\mathrm{m/s}, 0.0062 + \mathrm{j}0.0371);$$
$$\boldsymbol{C}_2 = (15\,\mathrm{MW}, 11.6331\,\mathrm{m/s}, 0.0168 + \mathrm{j}0.0990);$$
$\boldsymbol{C}_3$ is nonexistence;
$Prob(\mathrm{match}) = 0.1262$.

Scenario 2:

$$\boldsymbol{C}_1 = (60\,\mathrm{MW}, 5.4138\,\mathrm{m/s}, 0.0051 + \mathrm{j}0.0306);$$
$$\boldsymbol{C}_2 = (30\,\mathrm{MW}, 9.9531\,\mathrm{m/s}, 0.0231 + \mathrm{j}0.1360);$$
$\boldsymbol{C}_3$ is nonexistence;
$Prob(\mathrm{match}) = 0.1068$.

Scenario 3:

$$\boldsymbol{C}_1 = (75\,\mathrm{MW}, 5.1804\,\mathrm{m/s}, 0.0066 + \mathrm{j}0.0392);$$
$$\boldsymbol{C}_2 = (15\,\mathrm{MW}, 11.5377\,\mathrm{m/s}, 0.0084 + \mathrm{j}0.0495);$$
$\boldsymbol{C}_3$ is nonexistence;
$Prob(\mathrm{match}) = 0.1009$.

STATE GRID
STATE GRID ELECTRIC POWER RESEARCH INSTITUTE

References

[1] Slootweg JG, Kling WL (2003) The impact of large scale wind power generation on power system oscillations. Electr Power Syst Res 67(1):9–20

[2] Muljadi E, Butterfield CP, Parsons B et al (2008) Effect of variable speed wind turbine generator on stability of a weak grid. IEEE Trans Energ Convers 22(1):29–36

[3] Mendonca A, Peas Lopes JA (2005) Impact of large scale wind power integration on small signal stability. In: Proceedings of the 2005 international conference on future power systems (FPS'05), Amsterdam, Netherlands, 16–18 Nov 2005, 5 pp

[4] Anaya-Lara O, Jenkins N, Ekanayake J et al (2009) Wind energy generation: modelling and control. Wiley, Chichester

[5] Pena R, Clare JC, Asher GM (1996) Doubly fed induction generator using back-to-back PWM converters and its application to variable-speed wind-energy generation. IEE P- Electr Power Appl 143(3):231–241

[6] Bu SQ, Du W, Wang HF (2013) Probabilistic analysis of small-signal rotor angle/voltage stability of large-scale AC/DC power system as affected by grid-connected offshore wind generation. IEEE Trans Power Syst 28(4):3712–3719

[7] Fernández LM, Jurado F, Saenz JR (2008) Aggregated dynamic model for wind farms with doubly fed induction generator wind turbines. Renew Energ 33(1):129–140

[8] Zhou HQ, Zhang MS, Xue YS et al (2012) A dynamic equivalent method for doubly-fed induction generator wind farm based on the Thevenin equivalent circuit. Autom Electr Power Syst 36(23):42–47 (in Chinese)

[9] Feijoo A, Cidrás J, Carrillo C (2000) A third order model for the doubly-fed induction machine. Electr Power Syst Res 56(2):121–127

[10] Taleb M, Akbaba M, Abdullah EA (1994) Aggregation of induction machines for power system dynamic studies. IEEE Trans Power Syst 9(4):2042–2048

[11] Kundur P (1994) Power system stability and control. McGraw-Hill, New York

[12] Yang LH, Xu Z, Østergaard J et al (2011) Oscillatory stability and eigenvalue sensitivity analysis of a DFIG wind turbine system. IEEE Trans Energ Conver 26(1):328–339

[13] Fan LL, Zhu CX, Miao ZX et al (2011) Modal analysis of a DFIG-based wind farm interfaced with a series compensated network. IEEE Trans Energ Conver 26(4):1010–1020

[14] Anderson PM, Fouad AA (2002) Power system stability and control, 2nd edn. Wiley-IEEE Press, New York

Haiqiang ZHOU received his Ph.D. degree in electrical engineering from Zhejiang University, Hangzhou, China, in 2003. Since then, he has been with Hohai University, Nanjing, China, where he became an associate professor. His research interests include large-scale power system modeling and stability analysis.

Ping JU received his B.Eng. and M.Sc. degrees in electrical engineering from Southeast University, Nanjing, China, in 1982 and 1985, respectively, and his Ph.D. degree in electrical engineering from Zhejiang University, Hangzhou, China, in 1988. He is now a professor of electrical engineering at the College of Electrical Engineering at Hohai University, Nanjing. Dr. Ju was an Alexander von Humboldt Research Fellow at the University of Dortmund, Dortmund, Germany.

Yusheng XUE received his Ph.D. degree in electrical engineering from the University of Liege (Belgium) in 1987. He became a member of the Chinese Academy of Engineering in 1995. He is now the Honorary President of State Grid Electric Power Research Institute at the State Grid Corporation of China. His research interests include nonlinear stability, control, and power system automation.

Jie ZHU received her B.Eng. degree in electrical engineering from Jiangsu Technology University, Zhenjiang, China, in 2012. She is currently pursuing a M.Sc. degree at Hohai University.